

# Overcoming Problems Caused by Offset Distance of Multiple Targets in Single-isocenter Volumetric Modulated Arc Therapy Planning for Stereotactic Radiosurgery

Takaaki Ito<sup>1,2</sup>, Kazuki Kubo<sup>1</sup>, Hajime Monzen<sup>1</sup>, Yuya Yanagi<sup>1</sup>, Kenji Nakamura<sup>1</sup>, Yusuke Sakai<sup>1</sup>, Yasumasa Nishimura<sup>3</sup>

<sup>1</sup>Department of Medical Physics, Graduate School of Medical Sciences, Kindai University, Osakasayama, Osaka, <sup>2</sup>Department of Radiological Technology, Kobe City Nishi Kobe Medical Center, Kobe, Hyogo, <sup>3</sup>Department of Radiation Oncology, Faculty of Medicine, Kindai University, Osakasayama, Osaka, Japan

## Abstract

**Purpose:** The purpose of the study is to investigate the impact of large target offset distances on the dose distribution and gamma passing rate (GPR) in single-isocenter multiple-target stereotactic radiosurgery (SIMT SRS) using volumetric modulated arc therapy (VMAT) with a flattening filter-free (FFF) beam from a linear accelerator. **Methods:** Two targets with a diameter of 1 cm were offset by “±2, ±4, and ±6 cm from the isocenter in a verification phantom for head SRS (20 Gy/fr). The VMAT plans were created using collimator angles that ensured the two targets did not share a leaf pair from the multi-leaf collimator. To evaluate the low-dose spread intermediate dose spill ( $R_{50\%}$ ), GPRs were measured with a criterion of 3%/2 mm using an electronic portal imaging device and evaluated using monitor unit (MU), modulation complexity score for VMAT (MCS<sub>v</sub>), and leaf travel (LT) parameters. **Results:** For offsets of 2, 4, and 6 cm, the respective parameters were:  $R_{50\%}$ ,  $4.75 \pm 0.36$ ,  $5.13 \pm 0.36$ , and  $5.11 \pm 0.33$ ; GPR, 95.01%, 93.82%, and 90.67%; MU,  $5893 \pm 186$ ,  $5825 \pm 286$ , and  $5810 \pm 396$ ; MCS<sub>v</sub>, 0.24, 0.16, and 0.13; and LT,  $189.21 \pm 36.04$ ,  $327.69 \pm 67.01$ , and  $430.39 \pm 114.34$  mm. There was a spread in the low-dose region from offsets of  $\geq 4$  cm and the GPR negatively correlated with LT ( $r = -0.762$ ). There was minimal correlation between GPR and MU or MCS<sub>v</sub>. **Conclusions:** In SIMT SRS VMAT plans with an FFF beam from a linear accelerator, target offsets of  $< 4$  cm from the isocenter can minimize the volume of the low-dose region receiving 10 Gy or more. During treatment planning, it is important to choose gantry, couch, and collimator angles that minimize LT and thereby improve the GPR.

**Keywords:** Multiple targets, offset, single-isocenter, stereotactic radiosurgery, volumetric-modulated arc therapy

Received on: 21-01-2023

Review completed on: 06-09-2023

Accepted on: 12-09-2023

Published on: 05-12-2023

## INTRODUCTION

Whole-brain radiotherapy has been widely used to treat multiple brain metastases. However, stereotactic radiosurgery (SRS) has recently been recommended for the treatment of this condition because it improves long-term survival.<sup>[1-3]</sup> The high radiation accuracy required for SRS means that multiple isocenters must be irradiated when using a linear accelerator.<sup>[4]</sup> More recently, to reduce patient burden and make more efficient use of equipment,<sup>[5,6]</sup> single-isocenter multiple-target (SIMT) SRS volumetric modulated arc therapy (VMAT) has enabled shorter irradiation time.<sup>[7-9]</sup>

A flattening filter-free (FFF) beam is commonly utilized in SIMT SRS VMAT as it can provide shorter irradiation time and steeper dose gradients than a flattening filter beam,<sup>[5,7,8,10]</sup>

resulting in a smaller radiation dose to healthy brain tissue.<sup>[10]</sup> However, in SIMT SRS VMAT planning, targets as small as approximately 1 cm in diameter can be offset from the isocenter by more than 6 cm,<sup>[11,12]</sup> which may complicate the multi-leaf collimator (MLC) motion and increase the monitor unit (MU) level and thus lead to reduced irradiation accuracy.<sup>[13]</sup> Ohira *et al.* reported that gamma passing rates (GPRs) with 3%/3 mm of all SRS VMAT plans for a single target using a linear accelerator were 100%, whereas these rates decreased

**Address for correspondence:** Dr. Hajime Monzen, Department of Medical Physics, Graduate School of Medical Sciences, Kindai University, 377-2 Onohigashi, Osakasayama 5898511, Osaka, Japan. E-mail: hmon@med.kindai.ac.jp

This is an open access journal, and articles are distributed under the terms of the Creative Commons Attribution-NonCommercial-ShareAlike 4.0 License, which allows others to remix, tweak, and build upon the work non-commercially, as long as appropriate credit is given and the new creations are licensed under the identical terms.

**For reprints contact:** WKHLRPMedknow\_reprints@wolterskluwer.com

**How to cite this article:** Ito T, Kubo K, Monzen H, Yanagi Y, Nakamura K, Sakai Y, *et al.* Overcoming problems caused by offset distance of multiple targets in single-isocenter volumetric modulated arc therapy planning for stereotactic radiosurgery. *J Med Phys* 2023;48:365-72.

### Access this article online

Quick Response Code:



Website:  
www.jmp.org.in

DOI:  
10.4103/jmp.jmp\_8\_23

to 90% for SIMT SRS VMAT plans.<sup>[14]</sup> Ohira *et al.* reasoned that the decreased GPRs may be the result of backscatter effects from the support arm of the electronic portal imaging device (EPID),<sup>[14]</sup> although the causes remain unknown and it is important for clinical treatment planners to determine them to improve SIMT SRS VMAT plans.

In this study, we clarified how large target offsets result in a spread of low-dose regions and deterioration of GPRs in a cylindrical phantom for SIMT SRS VMAT plans with an FFF beam from a linear accelerator. Furthermore, the pitfalls arising from large target offsets and their consequences for clinical practice are discussed.

## METHODS

### Volumetric-modulated arc therapy planning with modified target offsets

In this study, a cylindrical phantom [MP, Toyo Medic, Tokyo, Japan; Figure 1] was imaged for head SRS verification and treatment planning using an Aquilion SP computed tomography (CT) system (Canon Medical Systems, Tochigi, Japan) with a slice thickness of 1 mm, resolution of 512 × 512 pixels, and field of view of 35 cm.

SIMT SRS VMAT plans were created using the Eclipse treatment planning system (TPS; version 15.6, Varian Medical Systems, Palo Alto, CA, USA). A TrueBeam linear accelerator (Varian Medical Systems, Palo Alto CA, USA) equipped with standard millennium MLCs and a 6 MV FFF beam (maximum achievable dose rate of 1400 MU/min). The whole MP phantom was automatically extracted by the TPS as “body”. The planning target volume (PTV) comprised two 1 cm-diameter regions with offsets of ±2, ±4, and ±6 cm along the RL, AP, and SI directions from the isocenter, which was set at the center of the MP phantom. As a minimum requirement in SIMT SRS for multiple brain metastases in our institution, the target size is ≥1 cm. In addition, considering the average head diameter, we have set the maximum offset at ±6 cm. An example of target offsets from the isocenter along the RL direction is shown in Figure 2. One full coplanar arc without couch rotation and three half-noncoplanar arcs with couch rotations of 315°, 45°, and 90° were set as shown in Figure 2a and Table 1.<sup>[14]</sup> In addition, the collimator angles were chosen so that the two targets did not share a leaf pair from the MLC [Table 1 and Figure 3].<sup>[12]</sup>

The prescription dose per fraction was 20 Gy/fr to 95% of the combined PTV of the two targets along each of the RL, AP, and SI directions.<sup>[15]</sup> Doses were calculated using the Acuros XB algorithm (Varian Medical Systems, Palo Alto, CA, USA) with heterogeneity correction on a 1 mm grid.<sup>[15]</sup> For each offset, five plans were created with the same optimization, and the calculated values were averaged. To achieve a steep dose gradient and high dose concentration,<sup>[15]</sup> the photon optimizer algorithm was used with a structure resolution of 1.25 mm and the following parameters: Maximum dose (Upper) to the PTV,<sup>[14]</sup> unrestricted; minimum dose (Lower) to the PTV,

20 Gy (priority = 200); normal tissue objective distance from target border, 0.1 cm; starting dose, 100%; end dose, 30%; fall-off factor, 0.45 (priority = 250). Furthermore, the optimization process used the jaw tracking technique,<sup>[12]</sup> which dynamically correlates the MLC aperture with the jaws during irradiation to reduce the size of low-dose regions by minimizing the leakage and transmission of the MLC leaves.<sup>[16]</sup>

Collimator, beam, and couch angles were set to ensure that the two targets did not share the leaf pair for each offset direction, thereby blocking dose leakage into normal tissue.

### Spread of low-dose regions

For all SIMT SRS VMAT plans and each target offset, dose-volume histogram (DVH) parameters including the homogeneity index (HI)<sup>[17]</sup> and Paddick’s conformity index (PCI)<sup>[18]</sup> of the PTV were evaluated, and the volume receiving 5 Gy or higher ( $V_{5Gy}$ ) and intermediate dose spill ( $R_{50\%}$ )<sup>[19]</sup> were used to evaluate the spread of the low-dose regions into off-target normal brain tissue.<sup>[20-22]</sup> We used  $R_{50\%}$  instead of the gradient index,<sup>[18]</sup> as both indices assess the spread of low-dose regions in normal brain tissue outside the target. The parameters HI, PCI, and  $R_{50\%}$  are defined as follows:

**Table 1: Beam arrangement for each offset direction (anterior-posterior, right-left, superior-inferior) of the target**

Gantry angle (°)	Couch angle (°)	Collimator angle (°)		
		Offset along the AP direction	Offset along the RL direction	Offset along the SI direction
179–181	0	90	90	0
181–0	315	90	0	0
0–179	45	90	0	0
179–0	90	90	0	90

AP: Anterior-posterior, RL: Right-left, SI: Superior-inferior

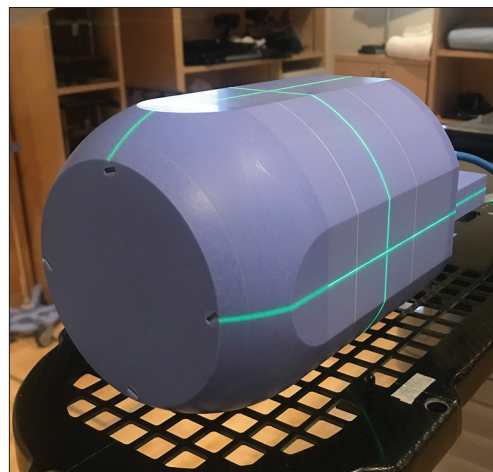


**Figure 1:** The phantom used in this study to verify treatment plans for stereotactic radiosurgery on the head

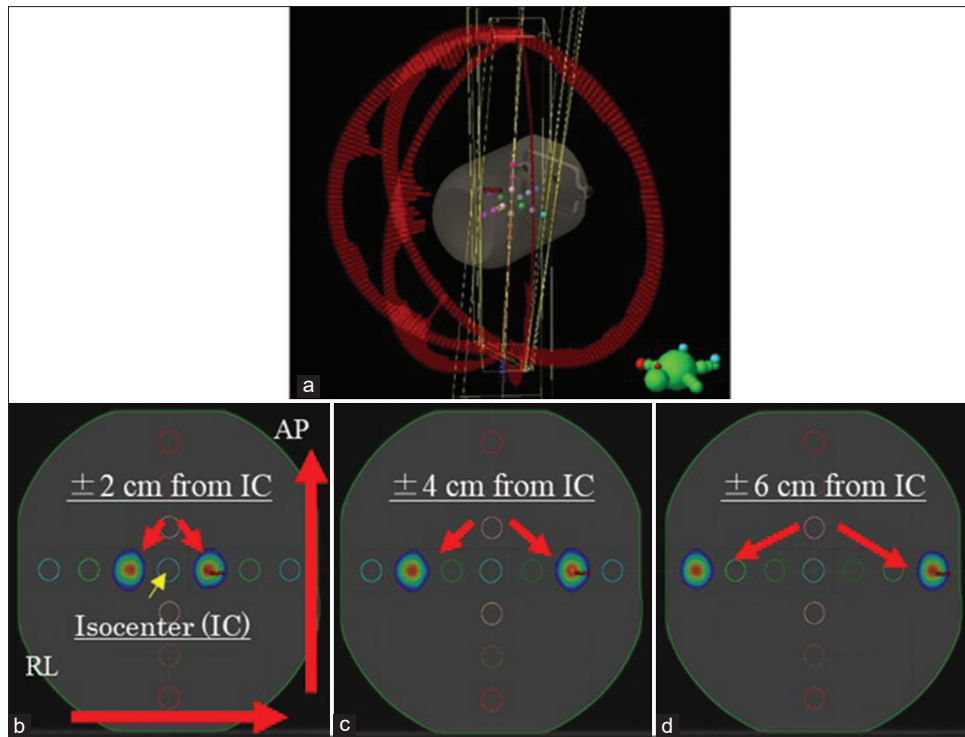


**Figure 2:** Beam arrangements and offset of the target from the isocenter (IC) along the RL direction. (a) Four arcs (one rotation at 0° couch angle and three noncoplanar beams at 315°, 45°, and 90° couch angles). (b) Offset of 2 cm along the RL direction. (c) Offset of 4 cm along the RL direction. (d) Offset of 6 cm along the RL direction

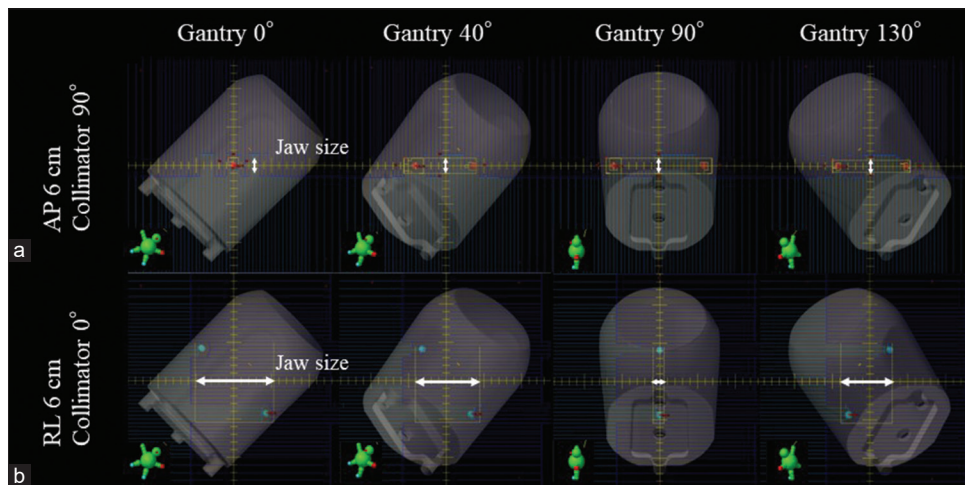


**Figure 3:** Multi-leaf collimator pattern at collimator angles chosen to minimize dose leakage into normal tissue using a half-arc beam at a couch rotation angle of 45°. (a) Offset of 6 cm along the AP direction (AP 6 cm). (b) Offset of 6 cm along the RL direction (RL 6 cm). The arrows show the jaw size

$$HI = D_{max} / D_{prescribed} \quad (1)$$

$$PCI = (TV_{PV})^2 / (TV \times PV) \quad (2)$$

$$R_{50\%} = V_{IDL50\%} / TV \quad (3)$$

where  $D_{prescribed}$  indicates the prescription dose and  $TV_{PV}$ ,  $TV$ ,  $PV$ , and  $V_{IDL50\%}$  represent the volume of the target covered by the prescription dose, the target volume, the prescription isodose volume, and the volume enclosed by the 50% isodose line, respectively.

### Inverse relationship between gamma passing rates and target offsets

Dosimetric accuracy was determined from the GPRs by comparing the fluence distribution measured using an EPID (aS1200 flat panel detector, Varian Medical Systems, Palo Alto, CA, USA) mounted on the linear accelerator with the fluence map calculated by the TPS.<sup>[23]</sup> Portal dosimetry is a method of fluence verification using EPID ignoring the couch and patient, irradiating without any scatterers and comparing the planned fluence to the delivered fluence measurement.<sup>[24]</sup>

Portal dosimetry is commonly used clinically for the verification of SIMT SRS VMAT.<sup>[14,25]</sup> The results of film and portal dosimetry for gamma analysis are consistent with each other at our institution. GPRs were obtained using the gantry and collimator angles shown in Table 1. The GPRs were obtained with a distance-to-agreement of 2 mm and dose differences of 3% and 2%. Our institution has a clinical target GPR of 95% with a 3%/2 mm threshold of 10%. If the above threshold is not achieved, the threshold is set to 25% and a GPR of 90% or more is allowed.<sup>[25]</sup> GPRs were evaluated at thresholds of 10% and 25%.<sup>[25]</sup> Portal dosimetry software (Varian Medical Systems) was used for data analysis.<sup>[23]</sup>

### Correlation between multi-leaf collimator performance and gamma passing rate

To identify the reasons that low GPRs result from large target offsets, MLC performance was evaluated using the following parameters: MU; modulation complexity score for VMAT ( $MCS_v$ );<sup>[26]</sup> and leaf travel (LT).<sup>[26]</sup>  $MCS_v$  was obtained for each control point (CP) of the arc (instead of the segments) from the change in MLC aperture and the LT normalized by the MU value at all CPs. The  $MCS_v$  for each CP was then averaged to obtain the overall  $MCS_v$ , which represents the complexity of the irradiation field geometry.<sup>[26]</sup> LT represents the average travel distance of all MLCs moving within the irradiation field defined by the collimator jaw.<sup>[26]</sup> Smaller values of  $MCS_v$  and larger values of LT and MU indicate more complex MLC motion. The MLC positions and MU at each CP were obtained from the DICOM-RT data file and each parameter was calculated using MATLAB (MathWorks, Natick, MA, USA). Furthermore, correlations between GPR (3%/2 mm threshold of 10%) and MLC performance were evaluated to understand why large target offsets cause low GPRs.

### Statistical analysis

The Mann–Whitney  $U$  test was used to compare DVH parameters, GPRs, and MLC parameters for each target offset. The statistical significance level was adjusted to 0.016 using Bonferroni correction to ensure statistical reliability in multiple comparison, taking into account the number of comparisons. The multiple comparison on the same dataset can increase the likelihood of obtaining statistically significant results by chance. Therefore, Bonferroni correction is commonly used to address this issue.<sup>[27]</sup> Statistical analyses were performed using the R analysis software (version 4.0.0, www.r-project.org). Analysis of correlations between MU,  $MCS_v$ , LT, and GPR was performed. The resulting Pearson's correlation ( $r$ ) was considered weak for  $r < 0.4$ , moderate for  $0.4 \leq r \leq 0.7$ , and strong for  $r > 0.7$ .<sup>[26]</sup>

## RESULTS

### Effect of target offset size on the spread of low-dose regions

Table 2 shows the HI, PCI,  $V_{5Gy}$ , and  $R_{50\%}$  parameters for each plan with the target offset along the RL, AP, and SI directions. There were no significant differences in HI and PCI at different

target offsets. In contrast,  $V_{5Gy}$  was significantly smaller at a 6 cm offset than at 4 cm, and  $R_{50\%}$  was significantly larger at 4 cm and 6 cm offsets than at a 2 cm offset.

### Effect of target offset size on gamma passing rate

Table 3 shows the GPRs measured using the EPID for each plan with target offsets along the RL, AP, and SI directions. The 6 cm offset yielded significantly smaller GPRs than the 2 cm offset for 3%/2 mm ( $P = 0.011$ ) and 2%/2 mm ( $P < 0.01$ ) thresholds of 10% [Table 3]. In addition, at the 3%/2 mm threshold of 10%, the GPRs were all above 90% at the 2 cm offset, while the lowest GPRs for the 4 cm and 6 cm offsets, both along the RL direction, were 87.7% and 80.6%, respectively. At the GPR threshold of 25%,<sup>[25]</sup> the average GPR for the 6 cm offset along the RL direction was 90.1%.

For all target offsets, the GPRs along the RL and SI directions were lower than those along the AP direction [ $P < 0.01$ ; Figure 4]. In addition, at the 3%/2 mm threshold of 10%, GPRs were above 90% for all offsets along the SI direction, whereas the GPR for a 6 cm offset along the RL direction was below 90% [Figure 4].

### Correlation between multi-leaf collimator performance and gamma passing rate

Table 4 shows the measured values of MU,  $MCS_v$ , and LT for each target offset. There were no significant differences in MU values for different target offsets. In contrast,  $MCS_v$  values for 4 cm and 6 cm offsets were significantly smaller than that for a 2 cm offset ( $P < 0.01$ ). In addition, larger target offsets resulted in significantly larger LT values ( $P < 0.01$ ).

Figure 5 shows the values of MU,  $MCS_v$ , and LT for each target offset direction. Smaller MU values were obtained for larger target offsets along the AP direction ( $P < 0.01$ ), and larger MU values were obtained for larger offsets along the SI direction ( $P < 0.01$ ). In addition,  $MCS_v$  was significantly larger for offsets of 4 cm and 6 cm along the SI direction compared with the AP and RL directions ( $P < 0.01$ ). In contrast, LT values were significantly lower for offsets of 4 cm and 6 cm

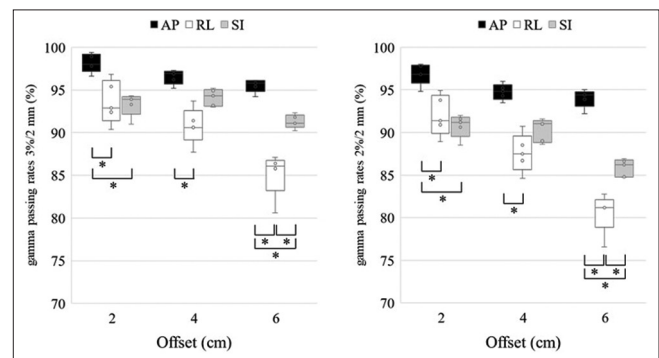


**Figure 4:** Gamma passing rates measured using portal dosimetry with a threshold of 10% for different target offsets along AP, RL, and SI directions. Black lines indicate the median of the data, and boxes range from the 1<sup>st</sup> to 3<sup>rd</sup> quartile. All points are plotted because the number of samples was small. ◦: Measured values, \*:  $P < 0.01$

**Table 2: Dose–volume histogram parameters for different target distance offsets**

DVH parameter	Plan				P value		
	Offset 0 cm	Offset 2 cm	Offset 4 cm	Offset 6 cm	2 cm versus 4 cm	2 cm versus 6 cm	4 cm versus 6 cm
HI	1.32±0.02	1.34±0.03	1.34±0.02	1.34±0.02	NS	NS	NS
PCI	0.92±0.00	0.92±0.00	0.91±0.01	0.91±0.01	NS	NS	NS
V <sub>5Gy</sub> (cm <sup>3</sup> )	8.35±1.73	19.17±2.74	20.24±1.18	18.51±0.90	NS	NS	<0.01
R <sub>50%</sub>	4.15±0.34	4.75±0.36	5.13±0.19	5.11±0.33	<0.01	<0.01	NS

Offset 0 cm is a single 1 cm target placed at the IC. HI: Homogeneity index, PCI: Paddick’s conformity index, V<sub>5Gy</sub>: Volume receiving 5 Gy or higher, R<sub>50%</sub>: Intermediate dose spill, NS: Not significant, IC: Isocenter

**Table 3: Gamma passing rates measured using portal dosimetry for different target offsets**

Offset (cm)	3%/2 mm (%) Th 10%				2%/2 mm (%) Th 10%			
	Mean	Maximum	Minimum	SD	Mean	Maximum	Minimum	SD
2	95.01	99.40	90.40	2.72	93.20	98.00	88.50	3.05
4	93.82	97.30	87.70	2.69	90.88	96.00	84.60	3.29
6	90.67	96.10	80.60	4.48	86.80	95.00	76.60	5.68
Offset (cm)	3%/2 mm (%) Th 25%				2%/2 mm (%) Th 25%			
	Mean	Maximum	Minimum	SD	Mean	Maximum	Minimum	SD
2	96.48	99.60	92.60	1.99	95.08	98.90	90.50	2.43
4	95.11	98.80	91.90	2.48	93.50	98.40	89.70	3.12
6	94.45	99.60	89.20	3.72	92.65	99.50	85.80	4.62

SD: Standard deviation, Th: Threshold

**Table 4: Multi-leaf collimator performance metrics for different target offsets**

	Plan				P value		
	Offset 0 cm	Offset 2 cm	Offset 4 cm	Offset 6 cm	2 cm versus 4 cm	2 cm versus 6 cm	4 cm versus 6 cm
MU	5754±345	5893±186	5825±286	5810±396	NS	NS	NS
MCS <sub>v</sub>	0.31±0.07	0.24±0.05	0.16±0.05	0.13±0.05	<0.01	<0.01	NS
LT (mm)	104.46±13.60	189.21±36.04	327.69±67.01	430.39±114.34	<0.01	<0.01	<0.01

Offset 0 cm is a single 1 cm target placed at the IC. MU: Monitor unit, MCS<sub>v</sub>: Modulation complexity score for VMAT, LT: Leaf travel, NS: Not significant, IC: Isocenter

along the AP direction compared with those along the RL and SI directions ( $P < 0.01$ ).

Furthermore, Figure 6 shows the correlations between GPR and MU, MCS<sub>v</sub>, and LT. There was a weak positive correlation between GPR and MCS<sub>v</sub> and a strong negative correlation between GPR and LT.

## DISCUSSION

For SIMT SRS VMAT planning using an FFF beam and a TrueBeam linear accelerator, this study showed that a larger target offset leads to an extended low-dose region and a smaller GPR. The dependency of V<sub>5Gy</sub>, R<sub>50%</sub>, MCS<sub>v</sub>, and LT on target volume and field size [Tables 2 and 4], we compared the results with those of a 2 cm offset as the reference, rather than using a zero offset. Larger target offsets resulted in an extended 50% prescribed dose region outside the targets (i.e., low-dose regions at V<sub>10Gy</sub>), and the value of V<sub>5Gy</sub> at a 6 cm offset was significantly lower than that at a 4 cm offset [Table 2], with the GPR increasing commensurately with the size of the

target offset [Table 3 and Figure 4]. Furthermore, larger target offsets resulted in a smaller MCS<sub>v</sub> and larger LT [Table 4 and Figure 5], and there was a strong negative correlation between GPR and LT [Figure 6]. Therefore, for SIMT SRS VMAT planning, larger target offsets are associated with a larger V<sub>10Gy</sub> low-dose region and larger LT. We suggest that the expansion of the low-dose region caused by leaf transmission, which could not be accurately taken into account in the dose calculation by the TPS, could have contributed to the smaller GPR [Figure 4]. Hence, LT is a marker of leaf transmission, and reducing the size of LT could therefore improve the DVH and GPR [Figure 6].

Notably, when dose calculations were performed under the same optimization constraints, larger target offsets had no impact on HI, PCI, or the dose delivered to the target but expanded the V<sub>10Gy</sub> region beyond the target [Table 2]. This low-dose region containing normal brain tissue has been reported to be an important predictor of radiation necrosis.<sup>[20-22]</sup> Prentou *et al.* suggested limiting the distance from the target to the isocenter to within 4 cm to prevent decreased target doses

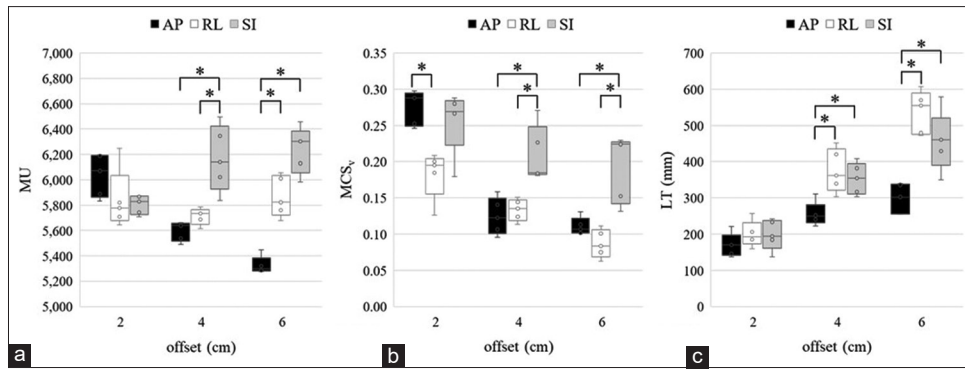


**Figure 5:** Multi-leaf collimator performance metrics evaluation for different target offsets along AP, RL, and SI directions, including (a) MU, (b) MCS<sub>v</sub> and (c) LT. Black lines indicate the median of the data, and boxes range from the 1st to 3rd quartile. All points are plotted because the number of samples was small. ○: Measured values, \*:  $P < 0.01$ , MU: Monitor unit, MCS<sub>v</sub>: Modulation complexity score for VMAT, LT: Leaf travel

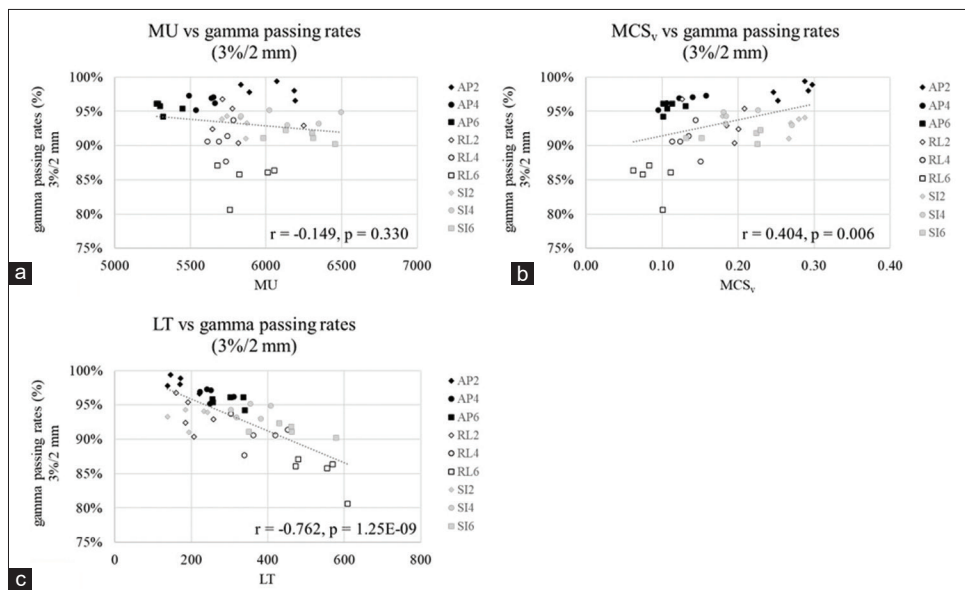


**Figure 6:** Relationships between the gamma passing rate with a threshold of 10% and (a) MU, (b) MCS<sub>v</sub>, and (c) LT. The diamonds, circles, and squares indicate values measured for target offsets of 2, 4, and 6 cm. Black, white, and gray symbols correspond to offsets along the AP, RL, and SI directions, respectively

caused by rotational errors in the patient setup, especially in SIMT SRS VMAT for small targets (<1 cm diameter). They also proposed dividing the isocenter into two to enhance robustness against rotational errors.<sup>[28]</sup> Our results show that a 4 cm target offset extends the  $V_{10Gy}$  low-dose region more than a 2 cm target offset. Therefore, we suggest that it is important to maintain a target distance from the isocenter should be <4 cm.

Ohira *et al.* reported that the MCS<sub>v</sub> parameter can predict the GPR in SRS VMAT planning for a single target,<sup>[29]</sup> although in SIMT SRS VMAT planning, there was no correlation between MCS<sub>v</sub> and GPR.<sup>[14]</sup> Similarly, our results showed only a weak positive correlation between MCS<sub>v</sub> and GPR [ $r = 0.404$ , Figure 6]. The complexity of MLC motions could not be evaluated using MCS<sub>v</sub> in SIMT SRS VMAT plans because MCS<sub>v</sub> was normalized by MU and because the larger the irradiation field size, the more nearly motionless MLCs were

taken into account in the calculation. Furthermore, the value of MU depended on the offset direction [Figure 5]. Therefore, the depth of the target position below the phantom surface and the characteristics of the FFF beam, which produces dose rates that are lower at the edges of the beam profile, were likely affected.

When two or more targets share a leaf pair, dose spillage into normal tissue occurs, which is referred to as island blocking.<sup>[30]</sup> With this effect in mind, we note that the GPR was smallest for target offsets along the RL direction and largest for offsets along the AP direction [Figure 4]. This might be attributed to the larger LT for target offsets along the RL and SI directions, which are caused by the increasing jaw size per gantry rotation for beams along the 315° and 45° couch angles [Figure 3b]. In contrast, for target offsets along the AP direction, the jaw size did not change and the

two targets were located on an axis perpendicular to the direction of MLC travel even though the gantry rotated with each beam, which resulted in no change in LT [Figure 3a]. Ohira *et al.* reported that changing the collimator angle setting could minimize the island-blocking problem by improving the irradiation efficiency and dose distribution and reducing MU, although it could not improve the GPR.<sup>[14]</sup> This was because the LT could not be shortened.

To the best of our knowledge, there have been no reports on the impact of large target offsets on dose distribution and GPR in SIMT SRS VMAT plans. It is important to ensure the quality of treatment planning because large target offsets along the RL direction significantly reduce the GPR and place limits on target offsets from the isocenter in SIMT SRS VMAT plans.<sup>[28,31,32]</sup> In addition, shortening the LT by setting gantry, couch, and collimator angles could reduce the extent of the low-dose region and improve the GPR. The ideal solution would be for the collimator to rotate in tandem with the gantry, although a more practical solution would be to: Narrow the range of gantry rotation angles (e.g., 60–120°) so that the targets share no leaf pairs and the jaw does not spread; change the collimator angle for each beam angle setting; and increase the number of beams to compensate for the resulting deterioration of the dose distribution.

In this study, we employed the widely used FFF beam in clinical with SIMT SRS for multiple brain metastases. However, it is important to note that FFF beams have nonflat profile shapes.<sup>[10]</sup> Therefore, when compared to a flattening filter beam, there is a possibility of varying impacts of offsets. Furthermore, a simple planning geometry (i.e., two 1 cm-diameter targets with symmetrical alignment to the isocenter) and a homogeneous phantom were used in this study to highlight the impact of target offset and eliminate other factors. It may be necessary to note the potential influence of clinical factors, such as heterogeneous phantoms and patient-specific CT images, on the results.

## CONCLUSIONS

In SIMT SRS VMAT plans with an FFF beam from a linear accelerator, target offsets of <4 cm from the isocenter can prevent the spread of the low-dose region receiving  $V_{10Gy}$ . Large target offsets result in correspondingly small GPRs, although offsets  $\leq 6$  cm are acceptable. During treatment planning, it is important to choose gantry, couch, and collimator angles that minimize LT and thereby improve the GPR.

## Acknowledgments

We would like to thank Edanz (<https://jp.edanz.com/ac>) for editing a draft of this manuscript.

## Financial support and sponsorship

Nil.

## Conflicts of interest

There are no conflicts of interest.

## REFERENCES

1. Tsao MN, Xu W, Wong RK, Lloyd N, Laperriere N, Sahgal A, *et al.* Whole brain radiotherapy for the treatment of newly diagnosed multiple brain metastases. *Cochrane Database Syst Rev* 2018;1:CD003869.
2. Yamamoto M, Serizawa T, Shuto T, Akabane A, Higuchi Y, Kawagishi J, *et al.* Stereotactic radiosurgery for patients with multiple brain metastases (JLGK0901): A multi-institutional prospective observational study. *Lancet Oncol* 2014;15:387-95.
3. Tsao MN, Rades D, Wirth A, Lo SS, Danielson BL, Gaspar LE, *et al.* Radiotherapeutic and surgical management for newly diagnosed brain metastasis(es): An American Society for Radiation Oncology evidence-based guideline. *Pract Radiat Oncol* 2012;2:210-25.
4. Clark GM, Popple RA, Young PE, Fiveash JB. Feasibility of single-isocenter volumetric modulated arc radiosurgery for treatment of multiple brain metastases. *Int J Radiat Oncol Biol Phys* 2010;76:296-302.
5. Ruggieri R, Naccarato S, Mazzola R, Ricchetti F, Corradini S, Fiorentino A, *et al.* Linac-based VMAT radiosurgery for multiple brain lesions: Comparison between a conventional multi-isocenter approach and a new dedicated mono-isocenter technique. *Radiat Oncol* 2018;13:38.
6. Guckenberger M, Roesch J, Baier K, Sweeney RA, Flentje M. Dosimetric consequences of translational and rotational errors in frame-less image-guided radiosurgery. *Radiat Oncol* 2012;7:63.
7. Thomas EM, Popple RA, Wu X, Clark GM, Markert JM, Guthrie BL, *et al.* Comparison of plan quality and delivery time between volumetric arc therapy (RapidArc) and Gamma Knife radiosurgery for multiple cranial metastases. *Neurosurgery* 2014;75:409-17.
8. Kadoya N, Abe Y, Kajikawa T, Ito K, Yamamoto T, Umezawa R, *et al.* Automated noncoplanar treatment planning strategy in stereotactic radiosurgery of multiple cranial metastases: HyperArc and CyberKnife dose distributions. *Med Dosim* 2019;44:394-400.
9. Khan MI, Rehman JU, Afzal M, Chow JC. Comparison of plan dosimetry on multi-targeted lung radiotherapy: A phantom-based computational study using IMRT and VMAT. *Nucl Eng Technol* 2022;54:3816-23.
10. Rieber J, Tonndorf-Martini E, Schramm O, Rhein B, Stefanowicz S, Kappes J, *et al.* Radiosurgery with flattening-filter-free techniques in the treatment of brain metastases: Plan comparison and early clinical evaluation. *Strahlenther Onkol* 2016;192:789-96.
11. Roper J, Chanyavanich V, Betzel G, Switchenko J, Dhabaan A. Single-isocenter multiple-target stereotactic radiosurgery: Risk of compromised coverage. *Int J Radiat Oncol Biol Phys* 2015;93:540-6.
12. Pokhrel D, Palmiero AN, Bernard ME, Clair WS. Dynamic conformal arcs-based single-isocenter VMAT planning technique for radiosurgery of multiple brain metastases. *Med Dosim* 2021;46:195-200.
13. Kamperis E, Kodona C, Hatzioannou K, Giannouzakos V. Complexity in radiation therapy: It's complicated. *Int J Radiat Oncol Biol Phys* 2020;106:182-4.
14. Ohira S, Sagawa T, Ueda Y, Inui S, Masaoka A, Akino Y, *et al.* Effect of collimator angle on HyperArc stereotactic radiosurgery planning for single and multiple brain metastases. *Med Dosim* 2020;45:85-91.
15. Lobb EC, Degnan M. Comparison of VMAT complexity-reduction strategies for single-target cranial radiosurgery with the Eclipse treatment planning system. *J Appl Clin Med Phys* 2020;21:97-108.
16. Feng Z, Wu H, Zhang Y, Zhang Y, Cheng J, Su X. Dosimetric comparison between jaw tracking and static jaw techniques in intensity-modulated radiotherapy. *Radiat Oncol* 2015;10:28.
17. Shaw E, Kline R, Gillin M, Souhami L, Hirschfeld A, Dinapoli R, *et al.* Radiation therapy oncology group: Radiosurgery quality assurance guidelines. *Int J Radiat Oncol Biol Phys* 1993;27:1231-9.
18. Paddick I, Lippitz B. A simple dose gradient measurement tool to complement the conformity index. *J Neurosurg* 2006;105 Suppl: 194-201.
19. Videtic GM, Hu C, Singh AK, Chang JY, Parker W, Olivier KR, *et al.* A randomized phase 2 study comparing 2 stereotactic body radiation therapy schedules for medically inoperable patients with stage I peripheral non-small cell lung cancer: NRG Oncology RTOG 0915 (NCCTG N0927). *Int J Radiat Oncol Biol Phys* 2015;93:757-64.
20. Voges J, Treuer H, Sturm V, Büchner C, Lehrke R, Kocher M, *et al.* Risk

- analysis of linear accelerator radiosurgery. *Int J Radiat Oncol Biol Phys* 1996;36:1055-63.
21. Blonigen BJ, Steinmetz RD, Levin L, Lamba MA, Warnick RE, Breneman JC. Irradiated volume as a predictor of brain radionecrosis after linear accelerator stereotactic radiosurgery. *Int J Radiat Oncol Biol Phys* 2010;77:996-1001.
  22. Minniti G, Clarke E, Lanzetta G, Osti MF, Trasimeni G, Bozzao A, *et al.* Stereotactic radiosurgery for brain metastases: Analysis of outcome and risk of brain radionecrosis. *Radiat Oncol* 2011;6:48.
  23. Hussein M, Rowshanfarzad P, Ebert MA, Nisbet A, Clark CH. A comparison of the gamma index analysis in various commercial IMRT/VMAT QA systems. *Radiother Oncol* 2013;109:370-6.
  24. Varian Medical Systems, Eclipse Photon and Electron Algorithms Reference Guide; 2017.
  25. Ballangrud Å, Kuo LC, Happersett L, Lim SB, Beal K, Yamada Y, *et al.* Institutional experience with SRS VMAT planning for multiple cranial metastases. *J Appl Clin Med Phys* 2018;19:176-83.
  26. Masi L, Doro R, Favuzza V, Cipressi S, Livi L. Impact of plan parameters on the dosimetric accuracy of volumetric modulated arc therapy. *Med Phys* 2013;40:071718.
  27. Kim JI, Ahn BS, Choi CH, Park JM, Park SY. Optimal collimator rotation based on the outline of multiple brain targets in VMAT. *Radiat Oncol* 2018;13:88.
  28. Prentou G, Pappas EP, Logothetis A, Koutsouveli E, Pantelis E, Papagiannis P, *et al.* Dosimetric impact of rotational errors on the quality of VMAT-SRS for multiple brain metastases: Comparison between single- and two-isocenter treatment planning techniques. *J Appl Clin Med Phys* 2020;21:32-44.
  29. Ohira S, Ueda Y, Isono M, Masaoka A, Hashimoto M, Miyazaki M, *et al.* Can clinically relevant dose errors in patient anatomy be detected by gamma passing rate or modulation complexity score in volumetric-modulated arc therapy for intracranial tumors? *J Radiat Res* 2017;58:685-92.
  30. Kang J, Ford EC, Smith K, Wong J, McNutt TR. A method for optimizing LINAC treatment geometry for volumetric modulated arc therapy of multiple brain metastases. *Med Phys* 2010;37:4146-54.
  31. Meeks SL, Mercado CE, Popple RA, Agazaryan N, Kaprealian T, Fiveash JB, *et al.* Practical considerations for single isocenter LINAC radiosurgery of multiple brain metastases. *Pract Radiat Oncol* 2022;12:195-9.
  32. Capaldi DP, Skinner LB, Dubrowski P, Yu AS. An integrated quality assurance phantom for frameless single-isocenter multitarget stereotactic radiosurgery. *Phys Med Biol* 2020;65:115006.